

Spiking Neural Network on Neuromorphic Hardware for Energy-Efficient Unidimensional SLAM

Guangzhi Tang, Arpit Shah, and Konstantinos P. Michmizos

Abstract—Energy-efficient simultaneous localization and mapping (SLAM) is crucial for mobile robots exploring unknown environments. The mammalian brain solves SLAM via a network of specialized neurons, exhibiting asynchronous computations and event-based communications, with very low energy consumption. We propose a brain-inspired spiking neural network (SNN) architecture that solves the unidimensional SLAM by introducing spike-based reference frame transformation, visual likelihood computation, and Bayesian inference. Our proposed SNN is seamlessly integrated into Intel’s Loihi neuromorphic processor, a non-Von Neumann hardware that mimics the brain’s computing paradigms. We performed comparative analyses for accuracy and energy-efficiency between our method and the GMapping algorithm, which is widely used in small environments. Our Loihi-based SNN architecture consumes 100 times less energy than GMapping run on a CPU while having comparable accuracy in head direction localization and map-generation. These results pave the way for extending our approach towards an energy-efficient SLAM that is applicable to Loihi-controlled mobile robots.

I. INTRODUCTION

Localization, knowing one’s pose, and mapping, knowing the positions of surrounding landmarks, are essential skills for both humans and robots as they navigate in unknown environments. The main challenge is to produce accurate estimates from noisy, error-prone cues, with robustness, efficiency, and adaptivity. Graph-based [1], [2] and filter-based approaches [3], [4] have solved the simultaneous localization and mapping (SLAM) problem by either optimizing a constrained graph or performing recursive Bayesian estimation. As they are tackling SLAM in a growing number of real-world applications, these approaches face increasing challenges for minimizing energy consumption.

Interestingly, efficient and highly accurate localization and mapping are “effortless” characteristics of mammalian brains [5]. Over the last few decades, a number of specialized neurons, including border cells, head direction cells, place cells, grid cells, and speed cells, have been found to be part of a brain network that solves localization and mapping [6] in an energy-efficient manner [7].

Large-scale neuromorphic processors [8], [9], [10], [11] have been proposed as a non-Von Neumann alternative to traditional computing hardware. These processors offer asynchronous event-based parallelism and relatively efficient solutions to many mobile robot applications [12], [13], [14]. Particularly, Intel’s Loihi processor [8] supports on-chip

synaptic learning, multilayer dendritic trees, and other brain-inspired components such as synaptic delays, homeostasis, and reward-based learning.

To leverage the disruptive potential of neuromorphic computing, we need to develop new algorithms that call for a bottom-up rethinking of our already developed solutions. Neuromorphic processors are designed to run Spiking Neural Networks (SNN), a specialized brain-inspired architecture where simulated neurons emulate the learning and computing principles of their biological counterparts. SNNs can introduce an orthogonal dimension to neural processing by adhering to the structure of the biological networks associated with the targeted tasks. Specifically, the brain’s spatial navigation and sensorimotor systems have inspired the design of SNNs that solved a number of problems in robotics [15], [16], [17]. Of particular interest for this study is an SNN inspired by the brain’s navigational system that enables a mobile robot to correct its estimate of pose and map of a simple environment, by periodically using a ground-truth signal [18].

In this paper, we present a biologically constrained SNN architecture which solves the unidimensional SLAM problem on Loihi, without depending on the external ground truth information. To do so, our proposed model determines the robot’s heading via spike-based recursive Bayesian inference of multisensory cues, namely visual and odometry information. We validated our implementation in both real-world and simulated environments, by comparing with the GMapping algorithm [3]. The SNN generated representations of the robot’s heading and mapped the environment with comparable performance to the baseline while consuming less than 1% of dynamic power.

II. METHOD

We developed a recursive SNN architecture that suggests a cue-integration connectome on Loihi to perform head direction localization and mapping. Inspired by the spatial navigation system found in the mammalian brain, the head direction and border cells in our network exhibited biologically realistic activity [6]. Our model had intrinsic asynchronous parallelism by incorporating spiking neurons, multi-compartmental dendritic trees, and plastic synapses, all of which are supported by Loihi.

Our model had 2 sensory spike rate-encoders and 5 sub-networks (Fig. 1). The odometry sensor and the RGB-Depth camera signals drove the neural activity of speed cells and sensory neurons encoding the angular speed and the distance to the nearest object, respectively. The Head Direction (HD) network received the input from the speed

*This work is supported by Intel’s INRC Grant Award

GT, AS and KM are with the Computational Brain Lab, Department of Computer Science, Rutgers University, New Jersey, USA. konstantinos.michmizos@cs.rutgers.edu

cells and represented the heading of the robot. The Reference Frame Transformation (RFT) network received the input from sensory neurons and generated allocentric distance representation in the world reference frame, as defined by the HD network. The Distance Mapping (DM) network learned the allocentric observations from the RFT network and formed the map of the robot’s surrounding environment. The Observation Likelihood (OL) network used the input from the DM network to compute the observation likelihood distribution of the robot’s heading based on the egocentric observation from sensory neurons. The Bayesian Inference (BI) network produced a near-optimal posterior of the robot’s heading and corrected the heading representation within the HD network. To do so, the BI network used the observation likelihood from the OL network and the odometry likelihood from the HD network. Each one of the networks is briefly described below.

A. Head Direction Network

Head direction cells in the HD network changed their spiking activity with respect to the current heading of the robot as follows. The HD network comprised of 75 neurons, each having a 5-degree resolution. We used the Continue Attractor Model to integrate angular speed and form a stable representation of the robot’s heading (Fig. 2a). The HD attractor state shifted either clockwise or counter-clockwise, depending on the robot’s rotation, with the help of transition neurons. There were two populations of such neurons to represent the two possible directions of rotation. Each transition neuron had a dendritic tree with one dendrite receiving spikes from the speed cell and the other from its corresponding head direction cell. The neuron fired when both dendrites were activated, thereby changing the HD attractor state.

B. Reference Frame Transformation Network

Border cells in the RFT network represented distance observations in the world reference frame (Fig. 2b). The sensory neurons represented discretized distances between the observable objects and the robot, in an egocentric manner. Similarly to our previous work [19], the RFT network used the HD activity to create an allocentric representation of the surrounding environment, therefore translating from egocentric observations to mapping. Other spike-based methods exist that perform reference frame transformation [20], [13], [21].

To perform the transformation in the RFT network, we leveraged the concurrent activity of sensory neurons and HD cells, as follows. Sensory neurons encoded the depth signal at the robot’s heading, as represented by HD cells. We created a group of border cells with the same preferred headings as the HD cells, allowing the border cells and HD cells to be on the same reference frame and have a one-to-one correspondence on preferred headings. Each border cell had a dendritic tree receiving spikes from HD cells and sensory neurons. A border cell fired maximally when the HD cells and sensory neurons connected to its dendritic tree were activated at the same time.

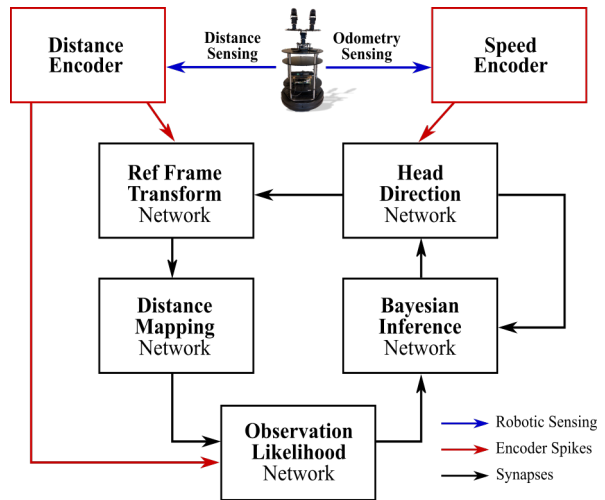


Fig. 1. Overall structure of the proposed SNN architecture.

C. Distance Mapping Network

The spiking activity of map neurons in the DM network represented the mapping of the robot’s surrounding environment (Fig. 2c). The learned map was stored on the synapses between a single place cell and all map neurons. These plastic synapses adhered to the Spike-Timing-Dependent Plasticity (STDP) rule. When the map (post-synaptic) neuron fired, the synaptic weight increased proportionally to the trace of the place cell’s (pre-synaptic) spikes, as described in the equation:

$$\delta w = A * x_1 * y_0 - B * u_k, \quad (1)$$

where the trace x_1 is the convolution of the pre-synaptic neuron’s spikes with a decaying exponential function; the factor y_0 changes from 0 to 1 whenever a post-synaptic neuron fires; the factor u_k is a decay factor which changes to 1 every k timesteps. During learning, border cells activated map neurons, and the location of the robot excited a place cell. A winner-take-all (WTA) structure in-between the map neurons, combined with the decay factor in the STDP rule, inhibited nearby map neurons and prevented overlearning.

D. Observation Likelihood Network

Likelihood neurons in the OL network changed their spiking activity based on the encoded distances and formed an observation likelihood distribution (Fig. 2d). The observation likelihood encoded the likelihoods of different headings based on the observed distance pattern. This distribution was multimodal when multiple similar distance patterns existed in the environment. This enabled the robot to estimate its heading without reference to its odometry sensor. The OL network is a spike-based alternative to the previously proposed scan matching methods [22], [23], which compute observation likelihoods based on visual observations.

The multilevel dendritic tree of the OL neuron generated, in an asynchronous manner, the likelihood activity by computing similarities between the depth signal and the map, as

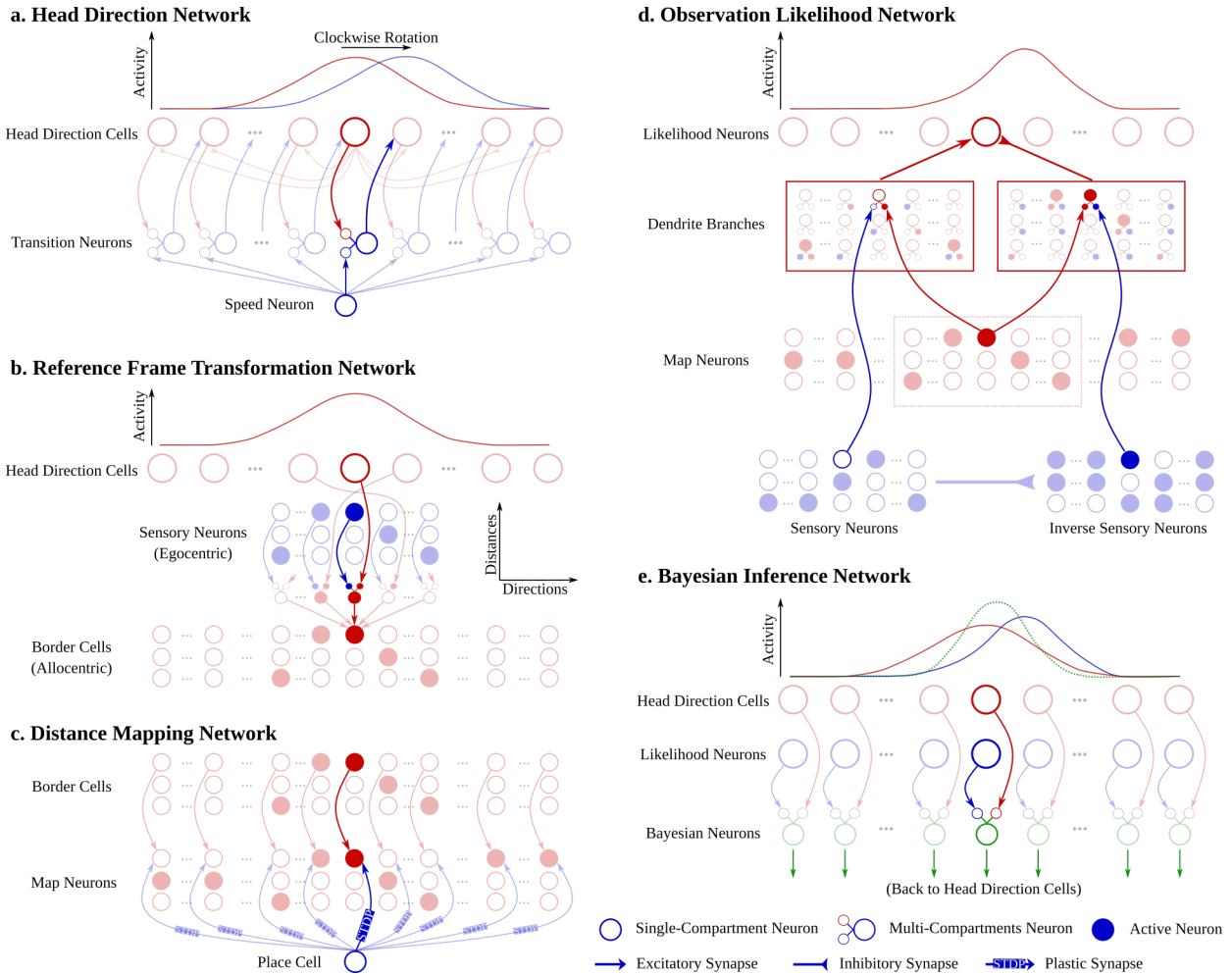


Fig. 2. Connectome of each sub-network in the proposed SNN architecture. a) Head direction network with one group of transition neurons. b) Reference frame transformation network with connections to a single border cell. c) Distance mapping network with connections to map neurons representing one of the three distances. d) Observation likelihood network with connections to one likelihood neuron. e) Bayesian inference network.

follows. Synaptic connections from map neurons to OL neurons formed spatial windows on the learned representations of the environment. We reinforced our prediction by considering the inverse of our learned observation represented by the inverse sensory neural population. The dendritic tree of a likelihood neuron had two main branches, one for comparing the distance pattern and the other for comparing the inverse distance pattern. The first and the second branch excited and inhibited the OL neurons, respectively, allowing them to increase their contrast in inferring the heading.

E. Bayesian Inference Network

Bayesian neurons in the BI network generated a posterior distribution from the likelihood functions (Fig. 2e), as defined in Equation 2:

$$p(s|d, o) \propto p(d|s)p(o|s)p(s), \quad (2)$$

where s is the heading of the robot, d is the distance observed, o is the odometry sensing. With a flat prior $p(s)$, the posterior distribution over the robot’s heading is proportional

to the product of two likelihood functions, $p(d|s)$ and $p(o|s)$, through Bayes’ theorem.

It is known that multiplying two Gaussian distributions produces another Gaussian distribution. This property enabled us to use dendritic trees to estimate the posterior distribution from likelihood distributions represented by the OL network and the HD network. Specifically, each Bayesian neuron had two dendritic compartments connected with its corresponding OL neuron and HD cell. The *PASS* dendritic operation on Loihi integrated the OL neuron voltage into a Bayesian neuron voltage when the HD cell spiked. Through this operation, the Bayesian neuron estimated the product of activities from the OL neuron and the HD cell.

F. Neuromorphic Realization in Loihi

We implemented our SNN architecture in one Loihi research chip. With a mesh layout, Loihi supports 128 neuromorphic cores with 1,024 compartments (primitive spiking neural units) in each core. Overall, a single chip provides up to 128k neurons and 128M synapses for building large-scale SNNs [8]. Our SNN architecture used 15,162 compartments

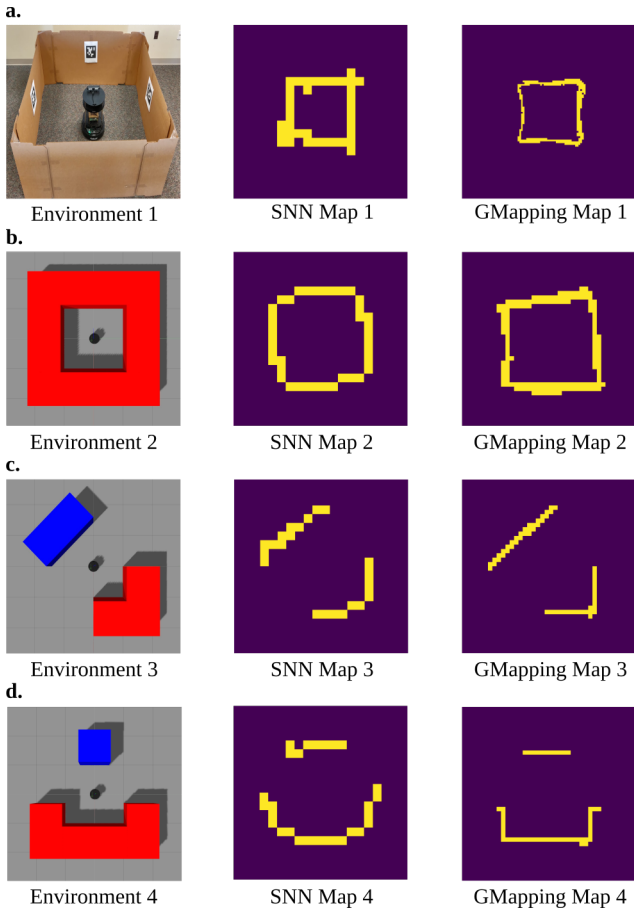


Fig. 3. (left column) Experimental environments; (middle column) Learned maps as represented by map neurons in our SNN architecture; (right column) Learned maps generated by the GMapping algorithm.

and 31,935 synapses distributed over 82 neuromorphic cores, slightly more than ten percent of the resources in a single Loihi research chip. When encoding the input from the distance observation, the encoder transformed all values to 3 discrete distance levels. Additionally, all neurons with HD receptive fields had a resolution of 5 degrees. For example, each sensory neuron encoded a single distance level for representing objects observable within 5 degrees.

III. EXPERIMENT AND RESULTS

A. Experimental Setup

We used a mobile robot equipped with an RGB-Depth camera, in both the real-world and Gazebo simulator, for validating our method. During all experiments, the robot rotated for 120 seconds with only angular velocity commands. We created 1 real-world and 3 simulated environments (Fig. 3). Environments 1 and 2 provide continuous observations with environment 2 being the simulated counterpart of the real-world environment. We further considered scenarios where non-continuous objects (Environments 3 and 4) were leaving gaps between themselves. In the simulated environments, we retrieved the ground truth of the robot’s heading directly from Gazebo model states. In the real-world environment, we used

the AprilTag detection system [24] and 4 AprilTag tags to determine sufficiently the ground truth values.

B. The Baseline Method

We chose the GMapping algorithm [3] as the baseline method solving the same unidimensional SLAM problem. To equally compare GMapping with our method, we limited GMapping to only the robot’s heading. For the real-world environment, GMapping built the map using a higher resolution of 0.04 meters and did scan-matching using all distance data from each update with a minimum score parameter of 700. For all simulated environments, GMapping built maps using a resolution of 0.1 meters and did scan-matching using 15 evenly distributed distance observations with a minimum score parameter of 10.

C. Localization and Mapping

We compared the heading from the HD cells with the ground truth values (Fig. 5). We conducted 5 experiments in the 4 environments and estimated the average error of headings to less than 15 degrees, for both our method and the GMapping. Given the 5 degrees resolution of the HD cells in our SNN, the error was in practice 1 to 3 neurons drifted in the attractor, which had up to 10 active neurons during the experiment. We observed a higher variance in the errors for environments 3 and 4 which is presumably due to the free space between the objects. When there was no object observed, the error increased temporarily until an object was within the range of the visual observation. Similarly to any filter-based approach on SLAM, as soon as an object was detected, there was a sharp correction which resulted in the drop of error (Figs. 5c and d).

We decoded the activity of the map neurons into a 20x20 gridmap representing a 4mx4m environment. Environments 1 and 2 had a square shape, and the maps generated by the SNN (Fig. 3a,b) successfully captured the repetitive distance pattern at the corners. Environments 3 and 4 had two objects with different shapes. The maps learned by our method (Fig 4c,d) reflected the differences between the two objects as perceived by the robot. We showcase how our proposed SNN can scale to mapping a more complicated environment by using more than one place cell in the DM network (Fig. 4).

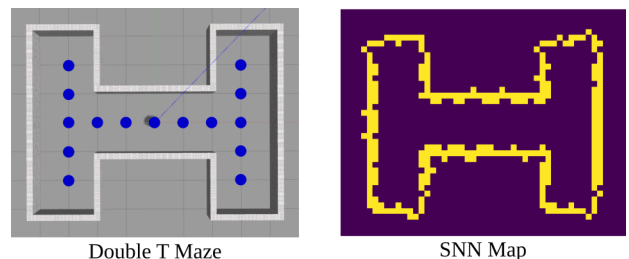


Fig. 4. Double T Maze environment to demonstrate scalability using multiple unidimensional maps, each for a single place cell in the DM network corresponding to a location in the maze (blue points). The learned map constructed by superimposing the maps from all place cells in our SNN architecture.

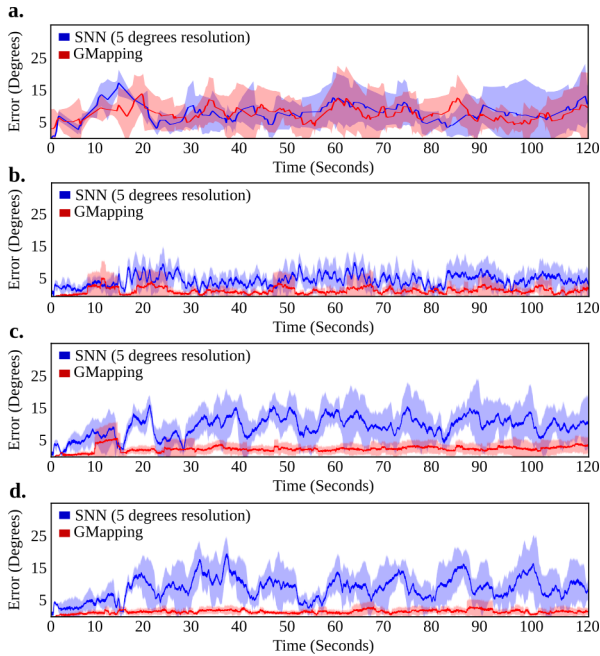


Fig. 5. Mean and STD of localization error over 5 experiments for both methods in a) Environment 1 (real-world environment), b) Environment 2, c) Environment 3, and d) Environment 4.

D. Observation Likelihood and Bayesian Inference

The activity of OL neurons captured the distinctive patterns in the learned environment. For instance, firing rates of OL neurons in Fig. 6a formed a bimodal distribution representing two possible headings due to the repetitive objects in Environment 4. We evaluated the activity of the Bayesian neurons by decoding the spikes from HD cells and OL neurons within a range of head directions into two Gaussian distributions, $N_1(\mu_1, \sigma_1^2)$ (red) and $N_2(\mu_2, \sigma_2^2)$ (blue) respectively. Equations (3) and (4) give the optimal posterior distribution $N_3(\mu_3, \sigma_3^2)$ (green) from these two likelihood distributions (Fig. 6a):

$$\mu_3 = \frac{\sigma_2^2}{\sigma_1^2 + \sigma_2^2} \mu_1 + \frac{\sigma_1^2}{\sigma_1^2 + \sigma_2^2} \mu_2 \quad (3)$$

$$\sigma_3^2 = \frac{1}{\frac{1}{\sigma_1^2} + \frac{1}{\sigma_2^2}} \quad (4)$$

We also computed the differences of the means and the standard deviations (STDs) between the decoded posterior distribution from Bayesian neurons and the optimal posterior distribution during runtime (Fig. 6b). During execution, the differences between the means and STDs were always less than 5 degrees, which is, in fact, the resolution of head direction in our SNN. The transient increase in the STD differences in Fig 6b was caused by the small resolution, constrained to 2 or 3 neurons, for representing the posterior distribution. Overall, the BI network generated near-optimal posterior distribution by performing spike-based Bayesian inference.

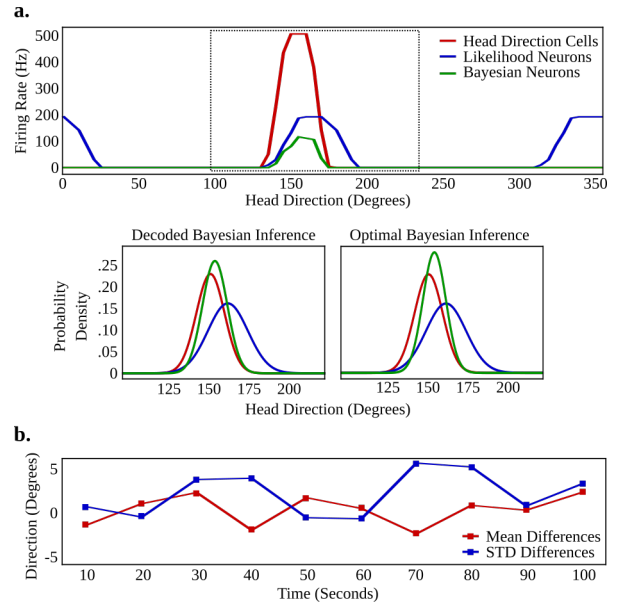


Fig. 6. Spike-based Bayesian inference. a) (upper panel) Neuronal activities within the BI network for Environment 4 and (bottom panel) comparison between the decoded and the optimal Bayesian inference results. b) Mean and STD differences between the decoded and the optimal posterior distribution during a single run in Environment 4.

E. Energy Efficiency

Our Loihi-based SNN architecture was much more energy efficient compared to GMapping running on a laptop CPU solving the same unidimensional SLAM problem (Fig. 7). Specifically, we evaluated the power consumption of our SNN using the Nahuku board, an 8-chip Loihi system, and GMapping using the Intel i7-4850HQ CPU. We measured the idle power of Loihi by setting all compartments to non-updating state in multiple 10,000 time-step runs and the idle power of the CPU by running only the operating system for 10 minutes. The running power of both methods was determined by averaging power measurements in 6 experiments.

Similarly to GMapping, our SNN architecture performed real-time data processing by only using 0.3 seconds for execution per wall-clock second, on average. This allowed us to compare the Loihi power consumption and the CPU power consumption against the same wall-clock time of the running robot (Fig. 7). We computed the dynamic power

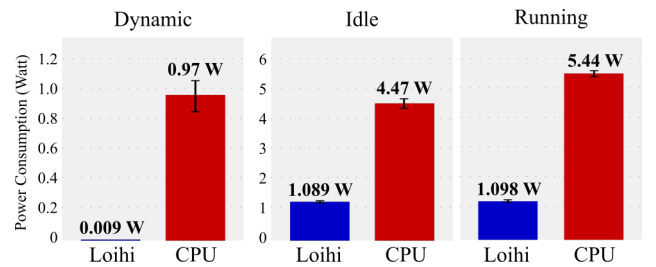


Fig. 7. Power consumption of our SNN architecture ran on Loihi and GMapping ran on CPU, solving the same unidimensional SLAM problem.

of each method by subtracting the idle power from the running power. An 8-chip Loihi board uses 4 times less power compared to a quad-core CPU in the idle state and our SNN running on Loihi was 100 times more energy efficient compared to GMapping running on a CPU in terms of dynamic power consumption. Since Loihi is at an early development stage, the power consumption, especially the idle power consumption, can be lowered further to 0.031 Watt in a more customized system [25] compared to the Nahuku board we utilized.

IV. DISCUSSION AND CONCLUSION

In this paper, we showed that an SNN architecture inspired by the brain's spatial navigation system and run on a neuromorphic processor can have similar accuracy and much lower power consumption, compared to a widely used method for solving the unidimensional SLAM problem. Although the error in the sparse environments was larger than GMapping, our proof-of-concept results can be improved by increasing the resolution or the stability of the HD network, to further demonstrate the validity of our proposed method as similarly accurate and much more efficient in terms of power consumption SLAM method. Similar to other solutions running on neuromorphic processors addressing speech recognition [25] and image processing [8], our solution currently yields results that are only comparable to the state-of-the-art methods that have been well-tuned to run on traditional Von Neumann CPUs.

For applications, such as planetary exploration and disaster rescue, where robots have limited recharging capabilities, energy efficiency is crucial. Our proposed neuromorphic approach provides an energy efficient solution towards the SLAM problem, which accounts for a large portion of the computational cost and its energy consumption.

Overall, our results form the basis for believing that the seamless integration of a neuromorphic algorithm and neuromorphic hardware might soon become a strong alternative, complementing a highly developed technology in mobile robot applications that require high energy efficiency. Although it probably requires a lot more small insights before it can outperform a highly developed technology, the fact that our Loihi-based SNN already gives unparalleled performance in energy is an indication that SNN-controlled robots are a direction worth exploring.

REFERENCES

- [1] R. Kümmerle, G. Grisetti, H. Strasdat, K. Konolige, and W. Burgard, "g2o: A general framework for graph optimization," in *Robotics and Automation (ICRA), 2011 IEEE International Conference on*. IEEE, 2011, pp. 3607–3613.
- [2] F. Dellaert, J. Carlson, V. Ila, K. Ni, and C. E. Thorpe, "Subgraph-preconditioned conjugate gradients for large scale slam," in *Intelligent Robots and Systems (IROS), 2010 IEEE/RSJ International Conference on*. IEEE, 2010, pp. 2566–2571.
- [3] G. Grisetti, C. Stachniss, and W. Burgard, "Improved techniques for grid mapping with rao-blackwellized particle filters," *IEEE transactions on Robotics*, vol. 23, no. 1, pp. 34–46, 2007.
- [4] J. Strom and E. Olson, "Occupancy grid rasterization in large environments for teams of robots," in *Intelligent Robots and Systems (IROS), 2011 IEEE/RSJ International Conference on*. IEEE, 2011, pp. 4271–4276.
- [5] S. Poulter, T. Hartley, and C. Lever, "The neurobiology of mammalian navigation," *Current Biology*, vol. 28, no. 17, pp. R1023–R1042, 2018.
- [6] R. M. Grieves and K. J. Jeffery, "The representation of space in the brain," *Behavioural processes*, vol. 135, pp. 113–131, 2017.
- [7] B. Sengupta and M. B. Stemmler, "Power consumption during neuronal computation," *Proceedings of the IEEE*, vol. 102, no. 5, pp. 738–750, 2014.
- [8] M. Davies, N. Srinivasa, T.-H. Lin, G. Chinya, Y. Cao, S. H. Choday, G. Dimou, P. Joshi, N. Imam, S. Jain, *et al.*, "Loihi: A neuromorphic manycore processor with on-chip learning," *IEEE Micro*, vol. 38, no. 1, pp. 82–99, 2018.
- [9] P. A. Merolla, J. V. Arthur, R. Alvarez-Icaza, A. S. Cassidy, J. Sawada, F. Akopyan, B. L. Jackson, N. Imam, C. Guo, Y. Nakamura, *et al.*, "A million spiking-neuron integrated circuit with a scalable communication network and interface," *Science*, vol. 345, no. 6197, pp. 668–673, 2014.
- [10] J. Schemmel, D. Brüderle, A. Gribbl, M. Hock, K. Meier, and S. Millner, "A wafer-scale neuromorphic hardware system for large-scale neural modeling," in *Circuits and systems (ISCAS), proceedings of 2010 IEEE international symposium on*. IEEE, 2010, pp. 1947–1950.
- [11] S. B. Furber, F. Galluppi, S. Temple, and L. A. Plana, "The spinnaker project," *Proceedings of the IEEE*, vol. 102, no. 5, pp. 652–665, 2014.
- [12] Y. Mei, Y.-H. Lu, Y. C. Hu, and C. G. Lee, "A case study of mobile robot's energy consumption and conservation techniques," in *Advanced Robotics, 2005. ICAR'05. Proceedings., 12th International Conference on*. IEEE, 2005, pp. 492–497.
- [13] H. Blum, A. Dietmüller, M. B. Milde, J. Conradt, G. Indiveri, and Y. Sandamirskaya, "A neuromorphic controller for a robotic vehicle equipped with a dynamic vision sensor," in *Robotics: Science and Systems*, 2017.
- [14] T. Hwu, J. Isbell, N. Oros, and J. Krichmar, "A self-driving robot using deep convolutional neural networks on neuromorphic hardware," in *2017 International Joint Conference on Neural Networks (IJCNN)*. IEEE, 2017, pp. 635–641.
- [15] Z. Bing, C. Meschede, K. Huang, G. Chen, F. Rohrbein, M. Akl, and A. Knoll, "End to end learning of spiking neural network based on r-stdp for a lane keeping vehicle," in *2018 IEEE International Conference on Robotics and Automation (ICRA)*. IEEE, 2018, pp. 1–8.
- [16] Z. Bing, C. Meschede, F. Röhrebein, K. Huang, and A. C. Knoll, "A survey of robotics control based on learning-inspired spiking neural networks," *Frontiers in neurorobotics*, vol. 12, p. 35, 2018.
- [17] T. Hwu, A. Y. Wang, N. Oros, and J. L. Krichmar, "Adaptive robot path planning using a spiking neuron algorithm with axonal delays," *IEEE Transactions on Cognitive and Developmental Systems*, vol. 10, no. 2, pp. 126–137, 2018.
- [18] R. Kreiser, A. Renner, Y. Sandamirskaya, and P. Pienroj, "Pose estimation and map formation with spiking neural networks: towards neuromorphic slam," in *2018 IEEE/RSJ International Conference on Intelligent Robots and Systems (IROS)*. IEEE, 2018, pp. 2159–2166.
- [19] G. Tang and K. P. Michmizos, "Gridbot: An autonomous robot controlled by a spiking neural network mimicking the brain's navigational system," in *Proceedings of the International Conference on Neuromorphic Systems*. ACM, 2018, p. 4.
- [20] S. Schneegans and G. Schöner, "A neural mechanism for coordinate transformation predicts pre-saccadic remapping," *Biological cybernetics*, vol. 106, no. 2, pp. 89–109, 2012.
- [21] A. Bicanski and N. Burgess, "A neural-level model of spatial memory and imagery," *eLife*, vol. 7, p. e33752, 2018.
- [22] A. Diosi and L. Kleeman, "Laser scan matching in polar coordinates with application to slam," in *Intelligent Robots and Systems, 2005.(IROS 2005). 2005 IEEE/RSJ International Conference on*. IEEE, 2005, pp. 3317–3322.
- [23] L. Montesano, J. Minguéz, and L. Montano, "Probabilistic scan matching for motion estimation in unstructured environments," in *Intelligent Robots and Systems, 2005.(IROS 2005). 2005 IEEE/RSJ International Conference on*. IEEE, 2005, pp. 3499–3504.
- [24] E. Olson, "AprilTag: A robust and flexible visual fiducial system," in *Robotics and Automation (ICRA), 2011 IEEE International Conference on*. IEEE, 2011, pp. 3400–3407.
- [25] P. Blouw, X. Choo, E. Hunsberger, and C. Eliasmith, "Benchmarking keyword spotting efficiency on neuromorphic hardware," *arXiv preprint arXiv:1812.01739*, 2018.